JOURNAL OF MATERIALS SCIENCE **35** (2000) 1459–1463

Syntheses and dielectric properties of perovskite ceramic system $PFW_{0.8-x}$·$PMN_{0.2}$·PFN_x

SUN-GON JUN, NAM-KYOUNG KIM*
Department of Inorganic Materials Engineering, Kyungpook National University, Taegu 702-701, Korea
E-mail: nkkim@kyungpook.ac.kr

$Pb[(Fe_{2/3}W_{1/3})_{0.8-x}(Mg_{1/3}Nb_{2/3})_{0.2}(Fe_{1/2}Nb_{1/2})_x]O_3$ system perovskite powders (phase purity >99%) were prepared via B-site precursor routes. Lattice parameter changes were analyzed in terms of B-site cation stoichiometries and sizes. Weak-field radio-frequency dielectric characteristics were investigated to verify the effect of composition modification on Curie temperatures and maximum dielectric constants. Unusual relaxation behaviors of frequency dispersion in the dielectric constant spectra at paraelectric region were observed.

1. Introduction

Lead iron tungstate ($Pb(Fe_{2/3}W_{1/3})O_3$, PFW) and lead iron niobate ($Pb(Fe_{1/2}Nb_{1/2})O_3$, PFN) possess very high maximum dielectric constants (1 kHz) of 20,000 [1, 2] and 24,000 [1, 2] at Curie temperatures of −95°C [3–6] and 112°C [1, 2, 7], respectively. Meanwhile, lead magnesium niobate ($Pb(Mg_{1/3}Nb_{2/3})O_3$, PMN), a prototype relaxor ferroelectric without any iron component, also has a very high dielectric constant (1 kHz) of 18,000 [1, 2, 8] at −10°C [1, 9]. In PFW [3–5, 9–11], PFN [3, 10, 11], and PMN [8, 10], B-site octahedral cations of Fe and W, Fe and Nb, and Mg and Nb are reported to be distributed in disorderly manners.

By the intrinsic high dielectric constants and low-temperature sinterability, PFW-PFN system (with some modifications in composition) has been studied intensively [11–17] as potential dielectric materials, which can replace traditionally-used $BaTiO_3$ [18], especially in multilayer-type capacitors. But the system had a detrimental problem of high dielectric losses by domain wall movement and conduction at low and high temperatures [19], which might possibly be reduced by substitution of low-loss PMN into the system. In another study of the PFW-PFN system [20], introduction of 20 mol% $Pb(Fe_{1/2}Ta_{1/2})O_3$ (PFT) increased the maximum dielectric constants by up to 50%. Like PFT, Curie temperature of PMN is also closer to room temperature than those of PFW and PFN, thus higher dielectric constants at room temperature can be expected by the introduction PMN.

In the present study, PMN-substituted PFW-PFN ceramic system was investigated in order to examine the effects of PMN on perovskite structure formation, lattice parameter changes, and dielectric characteristics. Moreover, it would also be interesting to observe the development of any structural ordering in the perovskite structure, as the ratios between the octahedral cations are 2:1 and 1:1 for PFW and PFN, whilst that of PMN is 1:2.

2. Experimental

Amount of PMN substituted to the PFW-PFN system was fixed to 20 mol%, resulting in a pseudobinary system of $(0.8-x)$PFW-0.2PMN-xPFN($x = 0.0$, 0.2, 0.4, 0.6 and 0.8). A B-site precursor method [21] (a new term which is conceptually identical to, but more inclusive than, the columbite process [22]) was used to synthesize perovskite powders of high phase yields. All of the raw materials used were oxides of high purity, >99%. Moisture contents of raw chemicals and synthesized B-site precursor oxides were measured and introduced into the batch calculations in order to maintain stoichiometries as closely to the normal compositions as possible.

To form multiple-cation B-site compositions of $[(Fe_{2/3}W_{1/3})_{0.8-x}(Mg_{1/3}Nb_{2/3})_{0.2}(Fe_{1/2}Nb_{1/2})_x]O_2$ (i.e., $[Mg^{2+}_{0.2/3}Fe^{3+}_{(3.2-x)/6}Nb^{5+}_{(0.8+3x)/6}W^{6+}_{(0.8-x)/3}]O_2$), powder mixtures were calcined at 950–1100°C for 2 h in air and were checked by x-ray diffraction (XRD) to identify the phases formed. Stoichiometric amounts of PbO was then added to the synthesized B-site precursors and the powder batches were calcined at 800–850°C for 2 h, followed by phase identification. Perovskite phase contents were determined by simple comparison between major peak intensities of (110) for perovskite and (222) for pyrochlore structures. The diffraction patterns were analyzed (with the pyrochlore peaks discarded) to obtain lattice parameters of a (pseudo)cubic perovskite structure.

The perovskite powders were formed isostatically into pellets and were fired at 950–1100°C for 1 h in

* Author to whom all correspondence should be addressed.

a double-enclosure crucible setup [23] to suppress lead volatilization. After polishing to make parallel sides, bulk densities of the ceramics were estimated geometrically, followed by Au sputtering as electrodes. Dielectric characteristics were examined using an impedance analyzer under a weak oscillation level of 1.0 V_{rms} at 1, 10, 100 and 1000 kHz on cooling.

3. Results and discussion

In Fig. 1 are XRD profiles of the B-site precursor system. Throughout the compositions, diffraction peaks of $MgNb_2O_6$ were not detected explicitly, so the $MgNb_2O_6$ components are believed to have dissolved into other host structures. At first glance, the whole patterns looked quite similar, which seemed to indicate the formation of continuous solid solutions. By considering the compositions, however, the situations are not so simple. Moreover, it was reported previously that Fe_2WO_6 and $FeNbO_4$ do not form complete solid solutions due to dissimilar structures [21]. At high values of x, the peaks matched quite satisfactorily with those of $FeNbO_4$. The sole detection of $FeNbO_4$ solid solutions can be attributed to the dissolution of $MgNb_2O_6$ into the $FeNbO_4$ structure. As a result, the diffraction peaks were shifted to lower angles by the influence of $MgNb_2O_6$ (Fig. 2). Meanwhile, most of the peaks at $x = 0.0$ (i.e., $[(Fe_{2/3}W_{1/3})_{0.8}(Mg_{1/3}Nb_{2/3})_{0.2}]O_2$) matched with those of Fe_2WO_6. However, an unnegligible peak at $\sim 24^\circ$ (marked by *) could be interpreted neither by Fe_2WO_6 nor by $MgNb_2O_6$, but only by the presence of $MgWO_4$ (Fig. 2). Other peaks of $MgWO_4$ were mostly overlapped by those of coexisting Fe_2WO_6 solid solution. During the formation of Fe_2WO_6 solid solution at low x's, therefore, a new phase of $MgWO_4$ seemed to have been formed. Coexistence of Fe_2WO_6 solid solution and $MgWO_4$ can be supported by the wider bases of the major diffraction peaks and also by the intensity reversal between two adjacent peaks at 54–55°. Formations of $MgWO_4$ were also reported in the system Fe_2WO_6-$MgNb_2O_6$ [24]. Like the case of high x's, diffraction angles at low x's were also shifted to lower values by the influences of $MgNb_2O_6$ as well as $MgWO_4$ (Fig. 2).

X-ray profiles of the $(0.8 - x)$PFW-0.2PMN-xPFN system powders are shown in Fig. 3, where development of a continuous series of perovskite solid solutions (phase yields of $>99\%$) is well demonstrated. Furthermore, absence of superlattice reflections revealed that the perovskite system did not develop any structural ordering among the octahedral cations. The disordered nature can be explained by the complex stoichiometries in the B-site compositions as well as rather small differences in ionic sizes [25], which were reported to be favorable conditions for the disordering [26, 27].

Lattice parameters of the perovskite structure are plotted Fig. 4. With increasing x (i.e., increasing PFN and decreasing PFW contents, or to be more specific, increasing Nb content and decreasing Fe and W contents, while that of Mg ion remained unchanged), the parameter of 0.3991 nm at $x = 0.0$ increased linearly to 0.4019 nm at $x = 0.8$. The steady increase in the parameters, satisfying the Vegard's law and confirming the formation of complete crystalline solutions,

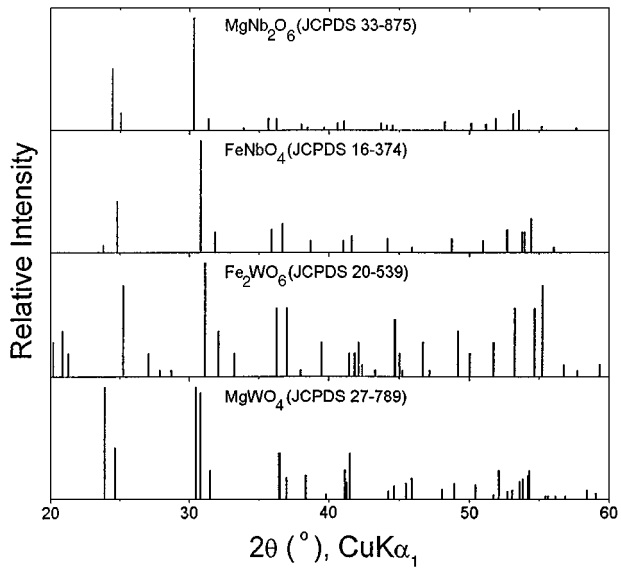

Figure 2 Comparison among JCPDS profiles of $MgNb_2O_6$, $FeNbO_4$, Fe_2WO_6 and $MgWO_4$.

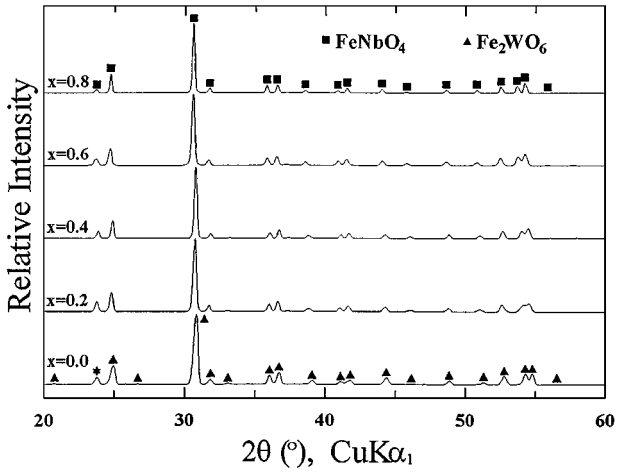

Figure 1 X-ray diffractograms of the B-site precursor system $[(Fe_{2/3}W_{1/3})_{0.8-x}\ (Mg_{1/3}Nb_{2/3})_{0.2}(Fe_{1/2}Nb_{1/2})_x]O_2$.

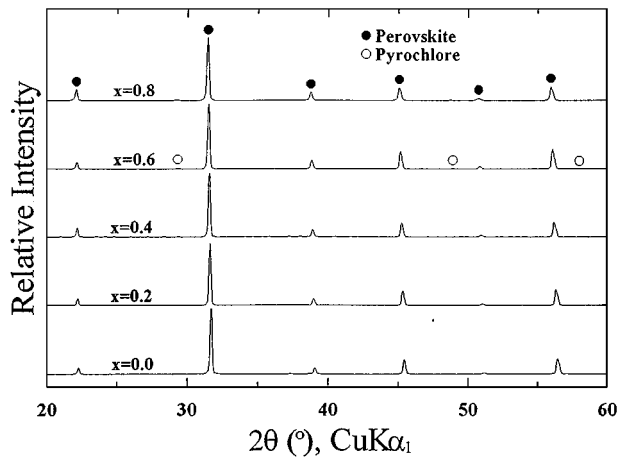

Figure 3 XRD patterns of the $(0.8 - x)$PFW$-$0.2PMN$-x$PFN system powders.

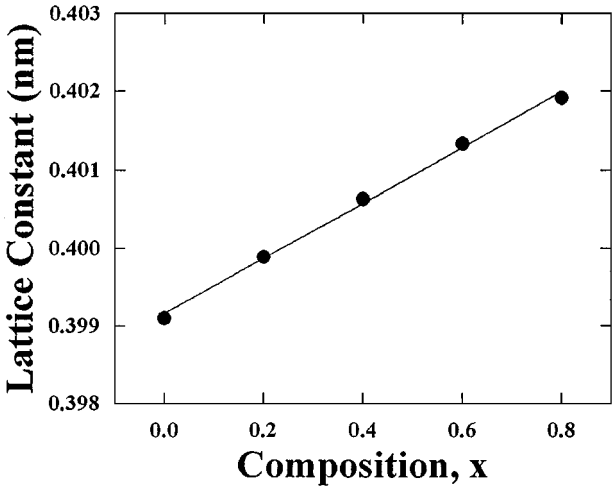

Figure 4 Variation of lattice parameters with composition change in the perovskite system.

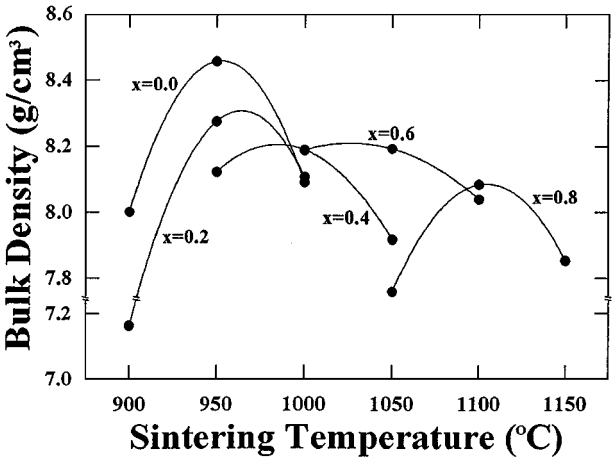

Figure 5 Bulk densities of ceramic specimen, as a function of sintering temperature.

can be understood by considering the octahedral ionic radii of Nb^{5+} versus Fe^{3+} and W^{6+}, 0.064 vs. 0.0645 and 0.060 nm [25], respectively. It was also observed that the increasing rate in the present system is very close to that in the systems of PFW-PFN [21] and $(0.8-x)$PFW-0.2PFT-xPFN [20], which can be explained by comparing detailed compositions of $Pb[Mg_{0.2/3}Fe_{(3.2-x)/6}Nb_{(0.8+3x)/6}W_{(0.8-x)/3}]O_3$ (present system), $Pb[Fe_{(4-x)/6}Nb_{x/2}W_{(1-x)/3}]O_3$ ($(1-x)$ PFW$-x$PFN system) and $Pb[Fe_{(3.8-x)/6}Ta_{0.1}Nb_{x/2}W_{(0.8-x)/3}]O_3$($(0.8-x)$PFW-0.2PFT-$x$PFN system). In the three systems, fractions of Nb, Fe and W ions vary at the same rates with composition change (i.e., $x/2$, $-x/6$ and $-x/3$, respectively), regardless of the presence of PMN or PFT. Hence, the perovskite lattices expanded accordingly.

Fig. 5 shows variations in bulk densities of the ceramics, as functions of sintering temperature and composition. In general, the bulk densities decreased with increasing x. Optimum sintering temperature of 950°C at $x = 0.0$ increased to 1100°C at $x = 0.8$, which is still much lower than 1200–1300°C of $BaTiO_3$ [2]. Meanwhile, relative densities of the sintered ceramics were 93–96% of theoretical, as calculated from the lattice parametres (Fig. 4) and molecular weights.

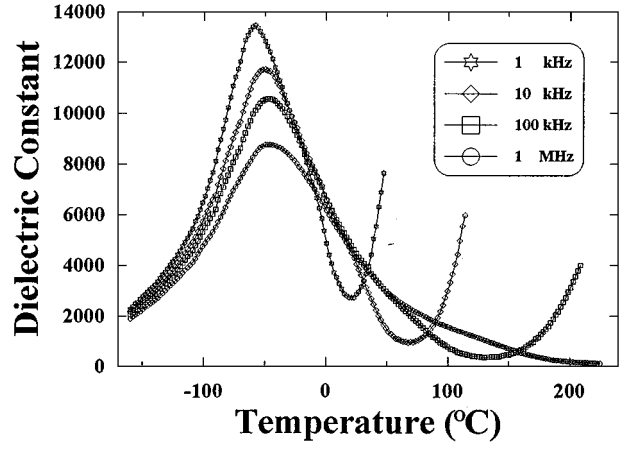

Figure 6 Representative dielectric constant spectra of $x = 0.2$.

Temperature- and frequency-dependent dielectric constants at composition $x = 0.2$ are shown in Fig. 6, where low-temperature spectra were typical of relaxor ferroelectrics (i.e., gradual increases in the Curie temperatures with increasing measurement frequency). At high temperatures above the phase transition range, however, the spectra deviated from the typical relaxor behaviors and showed faster decline in the dielectric constant to values lower than those at higher frequencies. Such unusual behaviors were also observed in several lead-based iron-containing complex perovskite compositions of PFW-PFT−PFN [28] and PFW-PMN−PFN [30], systems but were not observable in other complex perovskites. After the rapid fall in the dielectric constants at the paraelectric region, the values increased again steeply (accompanying sharp increases in dielectric losses), which were reportedly attributed to the conduction phenomena induced from space-charge polarization [29, 31–33], rather than to the intrinsic ferroelectric contribution. The rapid decline in dielectric constants above the phase transition may then also be related with the space-charge phenomena (which is prone to occur at low frequencies [34]), as the lower the measurement frequency, the steeper the decline and the lower the temperature of dielectric constant minimum. Dielectric spectra of other compositions in the perovskite system were similar too, Therefore, the intention to reduce the dielectric losses in the PFW-PFN system by introducing PMN turned out to be unsuccessful. In other words, PMN substitution by 20 mol% does not seem to be sufficient enough to reduce the high losses in the PFW-PFN system.

Dielectric constant spectra of the entire compositions are contrasted in Fig. 7. The dielectric peak at $x = 0.8$ was rather sharp and looked more like a first-order phase transition in $BaTiO_3$. At $x = 0.6$, the peak became less sharper, but still retained the first-order characters (e.g., slow increase in the dielectric constants, followed by a sudden rise at arround −25°C). The spectrum also showed a broad shoulder at ferroelectric-side of the peak, the mechanism behind which need to be investigated further. The sharp modes in the phase transitions at compositions of high x's are believed to be influenced by the component of PFN, which is reported to show first-order-like dielectric constant peak with a small degree of frequency relaxation [12, 21]. With

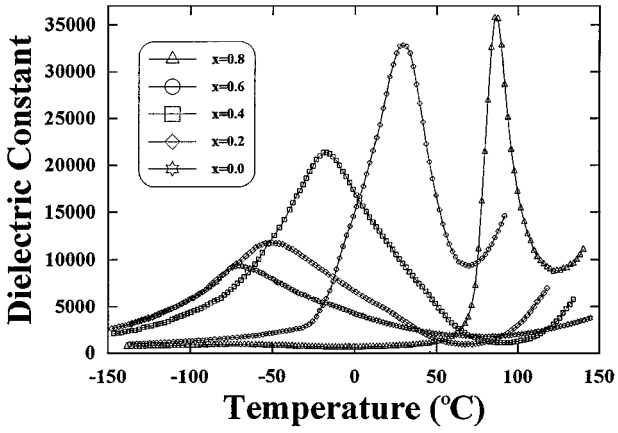

Figure 7 Dielectric constant spectra of the whole compositions in the perovskite system (10 kHz).

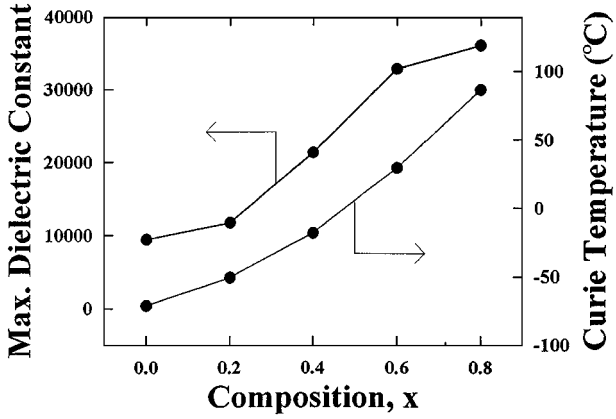

Figure 8 Maximum dielectric constants and Curie temperatures versus composition (10 kHz).

further decrease in x, the spectra became broader and smaller in peak heights, hence diffuse nature in phase transitions became pronounced.

Variations of maximum dielectric constant and Curie temperature are plotted in Fig. 8 against composition. The Curie temperature increased steadily from -71°C ($x = 0.0$) to 87°C ($x = 0.8$) which again proves the formation of perovskite solid solutions. In contrast, the maximum dielectric constant increased rather sharply at $0.2 \leq x \leq 0.6$, but only slightly at other composition range. Meanwhile, Curie temperature difference (10 kHz) between the end components in the present system was 158°C, whereas that in the PFW-PFN system was 188°C [21]. Hence substitution with 20 mol% PMN into the PFW-PFN system reduced the Curie temperature difference by ~16%. Such a reduction resulted from the presence of PMN, which raised and lowered the Curie temperatures of PFW- and PFN-rich compositions, respectively.

4. Summary

In the B-site precursor system $[(Fe_{2/3}W_{1/3})_{0.8-x}(Mg_{1/3}Nb_{2/3})_{0.2}(Fe_{1/2}Nb_{1/2})_x]O_2$, $MgNb_2O_6$ components dissolved into other structures to form solid solutions. Besides the solid solutions, however, a new phase of $MgWO_4$ was detected at low x's of Fe_2WO_6-rich compositions. Meanwhile, the system $(0.8-x)$PFW-0.2PMN$-x$PFN formed a continuous series of solid solutions of a disordered perovskite structure. Lattice parameters varied linearly with composition change, which was explained by the systematic increase in Nb content and decreases in Fe and W contents. Dielectric constant spectra of the system ceramics were of typical relaxors in the ferroelectric region, but unusual relaxation behaviors were observed after the phase transitions, which was interpreted by the space-charge polarization phenomena. Diffuse modes in the dielectric constant spectra at PFW-rich compositions became sharper and narrower with increasing PFN content, due to the intrinsic first-order-like phase transition nature in PFN. With increasing PFN, Curie temperatures increased steadily, whilst maximum dielectric constants increased at somewhat irregular rates.

Acknowledgements

This work was supported by the Korea Science and Engineering Foundation (KOSEF) through the Center for Interface Science and Engineering of Materials (CISEM) at Korea Advanced Institute of Science and Technology (KAIST).

References

1. Y. SAKABE, in "Proceedings of the MRS International Meeting on Advanced Materials, Tokyo, May 1988," edited by M. Doyama, S. Somiya and R. P. H. Chang (MRS) p. 119.
2. Y. YAMASHITA, *Am. Ceram. Soc. Bull.* **73** (1994) 74.
3. V. A. BOKOV, I. E. MYL'NIKOVA and G. A. SMOLENSKII, *Sov. Phys. JETP* **15** (1962) 447.
4. G. A. SMOLENSKII and V. A. BOKOV, *J. Appl. Phys.* **35** (1964) 915.
5. YU. E. ROGINSKAYA, YU. N. VENEVTSEV and G. S. ZHDANOV, *Sov. Phys. JETP* **21** (1965) 817.
6. S. M. SKINNER, *IEEE Trans. Parts, Materials and Packaging* **PMP-6** (1970) 68.
7. G. A. SMOLENSKII, A. I. AGRANOVSKAYA, S. N. POPOV and V. A. ISUPOV, *Sov. Phys.-Tech. Phys.* **3** (1958) 1981.
8. V. A. BOKOV and I. E. MYL'NIKOVA, *Sov. Phys.-Solid State* **3** (1961) 613.
9. I. G. ISMAILZADE, *Sov. Phys. Cryst.* **5** (1960) 292.
10. A. I. AGRANOVSKAYA, *Bull. Acad. Sci. USSR, Phys. Ser.* **24** (1960) 1271.
11. M. YONEZAWA, K. UTSUMI and T. OHNO, in Proceedings of the 1st Meeting on Ferroelectric Materials and Their Applications, 1977, p. 297.
12. H. TAKAMIZAWA, K. UTSUMI, M. YONEZAWA and T. OHNO, *IEEE Trans. CHMT* **CHMT-4** (1981) 345.
13. M. YONEZAWA, *Am. Ceram. Soc. Bull.* **62** (1983) 1375.
14. K. UTSUMI, Y. SHIMADA, H. TAKAMIZAWA, S. FUJII and S. NANAMATSU, in 34th Electronic Components Conf., 1984, p. 433.
15. H. TAKAHARA and K. KIUCHI, *Adv. Ceram. Mater.* **1** (1986) 346.
16. S.-L. FU and G.-F. CHEN, *Am. Ceram. Soc. Bull.* **66** (1987) 1397.
17. G. F. CHEN and S.-L. FU, *J. Mater. Sci.* **23** (1988) 3258.
18. A. RAE, *Am. Ceram. Soc. Bull.* **75** (1996) 108.
19. K. SAKATA and H. TAKAHARA, *Jpn. J. Appl. Phys.* **Suppl. 26–2** (1987) 83.
20. B.-H. LEE, K.-K. MIN and N.-K. KIM, *J. Mater. Sci.* **35** (2000) 197.
21. B.-H. LEE, N.-K. KIM, J.-J. KIM and S.-H. CHO, *Ferroelectrics* **211** (1998) 233.
22. S. L. SWARTZ and T. R. SHROUT, *Mater. Res. Bull.* **17** (1982) 1245.

23. M.-C. CHAE, N.-K. KIM, J.-J. KIM and S.-H. CHO, *Ferroelectrics* **211** (1998) 25.
24. S.-G. JUN and N.-K. KIM and B.-K LEE, *J. Mater. Sci*., in press.
25. R. D. SHANNON, *Acta Cryst.* **A32** (1976) 751.
26. N. SETTER and L. E. CROSS, *J. Mater. Sci*. **15** (1980) 2478.
27. M. P. HARMER, J. CHEN, P. PENG, H. M. CHAN and D. M. SMYTH, *Ferroelectrics* **97** (1989) 263.
28. B.-H. LEE, N.-K. KIM and S. H. LEE, *Ferroelectrics*, in press.
29. S.-G. JUN, N.-K. KIM, J.-J. KIM and S.-H. CHO, *J. Kor. Phys. Soc*. **32 Suppl**.(1998) S1002.
30. S.-G. JUN and N.-K. KIM, *Mater. Res. Bull*. **34** (1999) 613.
31. T. R. SHROUT, S. L. SWARTZ and M. J. HAUN, *Am. Ceram. Soc. Bull*. **63** (1984) 808.
32. N. K. KIM and D. A. PAYNE, *J. Mater. Res*. **5** (1990) 2045.
33. N. ICHINOSE and N. KATO, *Jpn. J. Appl. Phys*. **33** (1994) 5423.
34. R. C. BUCHANAN, "Ceramic Materials for Electronics: Processing, Properties, and Applications," 2nd ed. (Marcel Dekker, New York, 1991) p. 39.

Received 3 April 1998
and accepted 30 September 1999